Catalysis Today 148 (2009) 206–211

Contents lists available at ScienceDirect

Catalysis Today

journal homepage: www.elsevier.com/locate/cattod

Solid-solution catalysts for CO_2 reforming of methane☆

Yun Hang Hu

Department of Materials Science and Engineering, Michigan Technological University, 1400 Townsend Drive, Houghton, MI 49931-1295, United States

ARTICLE INFO

Article history:
Available online 21 August 2009

Keywords:
CO_2 reforming
CH_4
NiO
CoO
MgO
Solid solution

ABSTRACT

One of the important developments in CO_2 reforming of methane is highly effective MgO-based solid-solution catalysts. Herein, their high activity and selectivity as well as excellent stability for CO_2 reforming of methane were briefly reviewed. How to inhibit carbon deposition via the formation of NiO–MgO or CoO–MgO solid solution was discussed. The reduction of NiO (or CoO) in the NiO–MgO (or CoO–MgO) solid solution is much more difficult than that of pure NiO (or CoO), which contributes to the formation of very small Ni particles to inhibit carbon deposition. It is generally recognized that the reduction of a metal oxide is determined by its metal–oxygen bond strength. Herein, however, it was showed that the reduction of a metal oxide is strongly dependent on both metal–oxygen bond strength of the metal oxide and the metal–metal bond strength of its metal product. Furthermore, it was proposed that a critical factor to control the reduction of NiO (or CoO) in the solid solution is the isolation effect that NiO (or CoO) is isolated by MgO, which inhibits the metal–metal bond formation during the reduction.

1. Introduction

In the 1980s, Keller and Bhasin reported the oxidative coupling of methane to give ethylene and ethane [1]. This work prompted numerous attempts to convert methane directly to ethylene and ethane [1] as well as other compounds [2]. However, the best result obtained in long-run tests has been a C_{2+} yield of only 15% for methane conversions of 15–40% at a temperature of 1270–1370 K and a pressure of 1–2 atm with a CH_4/O_2 molar ratio of 5–10 [3]. In the early 1990s, a consensus emerged that it would be difficult to achieve a significantly better result than that mentioned above for the oxidative coupling to become an economical industrial process. This is because the formation of CO_2, instead of more desirable products (such as ethylene and ethane), is favored thermodynamically when the reaction of methane and oxygen is fast enough to be of practical interest at temperatures above 973 K. Consequently, in the early 1990s, the emphasis in research on CH_4 conversion returned to three indirect processes producing synthesis gas [4–8]: steam reforming (Eq. (1)), partial oxidation (Eq. (2)), and CO_2 reforming (Eq. (3)):

$$CH_4 + H_2O \rightarrow CO + 3H_2, \quad \Delta H^0_{298} = 206\ \text{kJ mol}^{-1} \tag{1}$$

$$CH_4 + (1/2)O_2 \rightarrow CO + 2H_2, \quad \Delta H^0_{298} = -36\ \text{kJ mol}^{-1} \tag{2}$$

$$CH_4 + CO_2 \rightarrow 2CO + 2H_2, \quad \Delta H^0_{298} = 247\ \text{kJ mol}^{-1} \tag{3}$$

The steam reforming is a commercial process, which was first developed by Standard Oil of New Jersey (current Exxon Moil Oil Corporation) [9]. Compared to the steam reforming of methane, the methane partial oxidation has two main advantages: (1) the partial oxidation is slightly exothermic instead of being strongly endothermic, and (2) the obtained H_2/CO ratio of about 2 is ideal for methanol synthesis and Fischer–Tropsch syntheses of short-chain hydrocarbons. However, the catalytic partial oxidation of methane requires a pure oxygen feed, which is prepared by expensive air separation.

CO_2 reforming, which is endothermic, can produce synthesis gas with a low H_2/CO ratio (1/1) that is suitable for the Fischer–Tropsch synthesis of long-chain hydrocarbons [10]. Furthermore, it can be carried out with natural gas from fields containing large amounts of CO_2 without the pre-separation of CO_2 from the feed. Because CO_2 is a greenhouse gas that causes warming of the earth, there are incentives for reducing its concentration in the atmosphere. Methane should be also considered as a greenhouse gas, because it can absorb 20 times more heat than CO_2. The CO_2 reforming of methane may provide a practical method for consumption of those two greenhouse gases. However, so far, no industrial technology for CO_2 reforming of methane has yet been developed. One of the main reasons is that no effective, economic catalysts have been discovered. When the conventional Ni-containing catalyst for steam reforming was used for CO_2

☆ Based on an invited plenary lecture by Y.H. Hu in the 10th International Conference on CO_2 Utilization, during May 17–21, 2009 in Tianjin, China.

E-mail address: yunhanghu@mtu.edu.

0920-5861/$ – see front matter © 2009 Elsevier B.V. All rights reserved.
doi:10.1016/j.cattod.2009.07.076

reforming, carbon deposits formed on the catalyst, which deactivated rapidly. A high molar ratio of CO_2 to CH_4 (≥ 3) could be used to reduce the carbon deposition by inhibiting CO disproportionation, but the selectivity to synthesis gas could become much lower than that for the stoichiometric CO_2 reforming ($CO_2/CH_4 = 1$). Therefore, the inhibition of carbon deposition without extra cost and loss of catalyst performance constitutes a major challenge for CO_2 reforming of methane. In the past 20 years, one of important developments in this area is MgO-based solid-solution catalysts [11–19]. In this article, the excellent catalytic performance of the solid-solution catalysts will be briefly reviewed. How to inhibit carbon deposition by using solid-solution catalysts will be discussed. Finally, the isolation effect of solid solution will be proposed as a critical factor to control the reduction of NiO in NiO/MgO solid solution, which plays an important role in inhibiting carbon deposition.

2. Catalytic performances of solid-solution catalysts

MgO is widely selected as a catalyst support due to its high thermal stability and low cost. The surface area of the metal oxide powders at high temperatures depends on their intrinsic properties, particularly melting point and phase transformation. MgO has a very high melting point (2850 °C), which can allow MgO to maintain a relatively large surface area at high temperatures compared to most oxides used as catalyst supports. Furthermore, MgO, NiO, and CoO have a face centered cubic structure with almost the same lattice parameters: 4.2112 Å for MgO, 4.1684 Å for NiO, and 4.2667 Å for CoO. As a result, the combination of MgO and NiO (or CoO) leads to the formation of solid solution (NiO–MgO or CoO–MgO). Several groups reported the excellent results of CO_2 reforming of methane in the presence of NiO–MgO and CoO–MgO solid-solution catalysts [11–19]. As shown in Fig. 1, a 20 wt.% NiO/MgO solid-solution catalyst for CO_2 reforming of methane, which was prepared by impregnation and was calcined at 1073 K, was reported [11]. The reduced solid-solution catalyst exhibited almost 100% conversion of CO_2, >91% conversion of CH_4, and >95% selectivities to CO and H_2 at 1063 K, atmospheric pressure, and the very high space velocity of 60,000 ml (g of catalyst)$^{-1}$ h^{-1} for a CH_4/CO_2 (1/1) feed (Fig. 1) [11]. The conversion and selectivity remained unchanged during the entire reaction time employed (120 h), indicating that the reduced NiO/MgO catalyst had a high stability. In contrast to MgO, the other alkaline-earth oxides, such as CaO, SrO, and BaO, were found to be poor supports for NiO, as they provided catalysts with low activities, selectivities, or stabilities [11]. Furthermore, although the reduced NiO/Al_2O_3 catalyst provided high initial conversions (CH_4, 91%; CO_2, 98%) and selectivities (>95% for both CO and H_2), it suffered a rapid carbon deposition, resulting in the complete plugging of the reactor after 6 h of reaction [12f]. It is reasonable to conclude that the excellent catalytic performance of NiO/MgO should be attributed to the formation of a solid solution [12]. The performance of NiO/MgO solid-solution catalysts are dependent on their composition, preparation conditions, and even the properties of the MgO [12]. High and constant H_2 and CO yields (>95%) occurred with NiO/MgO catalysts having NiO contents between 9.2 and 28.6 wt.% [12g]. No activity was observed, however, for a NiO content of 4.8 wt.%. At the high NiO content of 50 wt.%, the CO yield decreased from 91 to 53% after 40 h due to carbon deposition. This indicates that too-small amounts of NiO in the NiO/MgO catalysts provided too-small numbers of Ni sites, and too-large amounts supplied numerous nickel metal particles that could easily sinter and generate large particles, which facilitated carbon deposition. Furthermore, the MgO surface area, pore size distribution, and lattice parameters exhibited significant effects on the performance of NiO/MgO solid-solution catalysts [12e].

It was reported that the addition of a noble metal could promote both the activity and the stability of NiO/MgO solid-solution catalysts [13e]. The resistance of the $Ni_{0.03}Mg_{0.97}O$ solid-solution catalyst to carbon deposition was retained by the bimetallic catalysts [13e]. The improved stability of the catalyst was attributed to the increased catalyst reducibility caused by noble metal promotion. Furthermore, the water treatment of the $Ni_{0.03}Mg_{0.97}O$ solid-solution catalyst increased the catalytic activity and stability for CO_2 reforming of CH_4 [13d]. This promoting effect was inferred to be the consequence of a structural rearrangement of the solid solution by the formation of nickel and magnesium hydroxides [13d]. Very recently, Liu and Ge et al. revealed the effect of water on CO_2 adsorption on γ-Al_2O_3 by using density functional theory (DFT) calculations [20]. Their interesting results would be useful for ones to explain the effect of water on CO_2 reforming of methane.

The catalytic performance of NiO/MgO solid-solution catalysts for CO_2 reforming of methane is also affected by reactor type [18]. It was found that the methane and CO_2 conversion in the fluidized bed reactor was higher than those in the fixed bed reactor over $Ni_{0.15}Mg_{0.85}O$ catalyst at a pressure of 1.0 MPa. It was suggested that the promoting effect of catalyst fluidization on the activity is related to the catalyst reducibility. The oxidized and deactivated catalyst can be reduced with the produced syngas and the

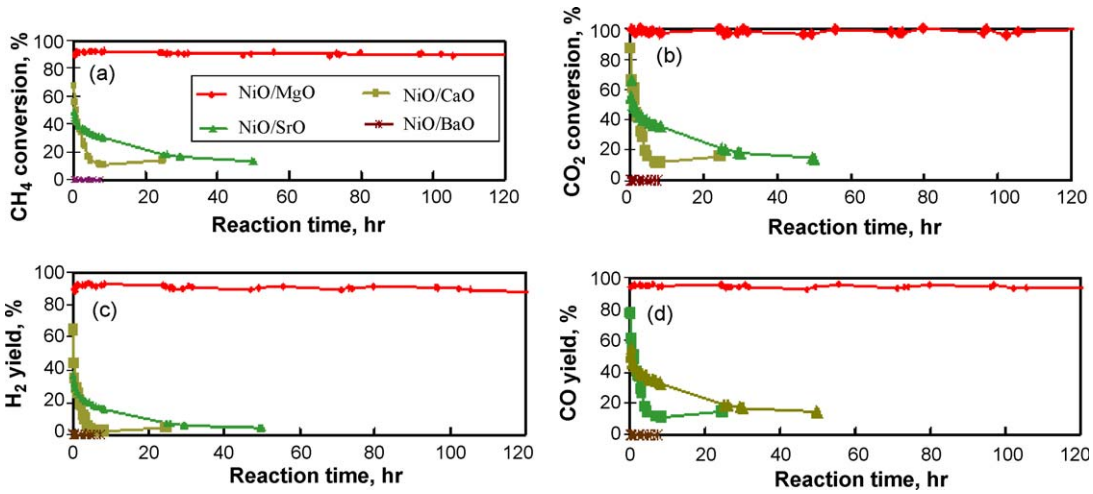

Fig. 1. CH_4 conversion (a), CO_2 conversion (b), H_2 yield (c), and CO yield (d) in the CO_2 reforming of CH_4 catalyzed by reduced 20 wt.% NiO/alkaline-earth metal oxides. Before reaction, each catalyst was reduced in flowing H_2 at 773 K for 14 h. Reaction conditions: pressure = 1 atm, T = 1063 K, CH_4/CO_2 = 1/1, GHSV = 60,000 ml (g of catalyst)$^{-1}$ h^{-1} [11].

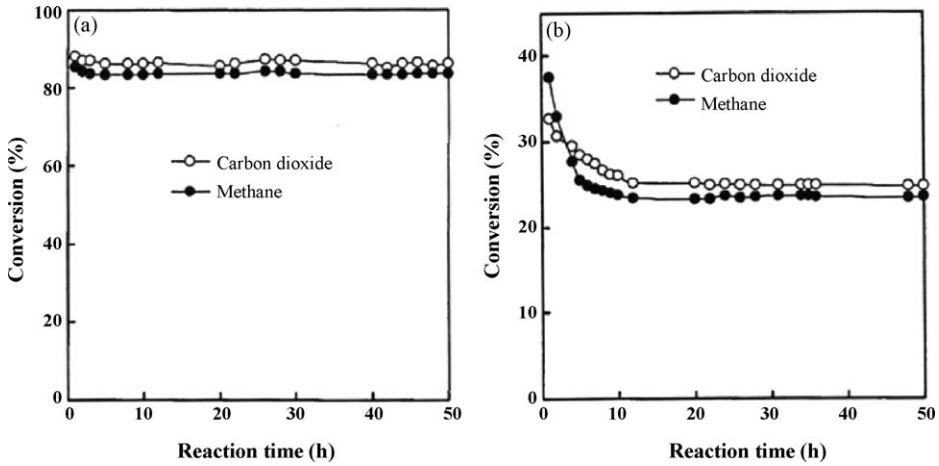

Fig. 2. CH_4 and CO_2 Conversions versus reaction time over 8.8 wt.% NiO/MgO catalyst at (a) atmospheric pressure and (b) high pressure of 1.5 MPa. Reaction condition: T = 1123 K, CH_4/CO_2 = 1, GHSV = 16,000 ml (g of catalyst)$^{-1}$ h^{-1}[15a].

reforming activity can be regenerated in the fluidized bed reactor during the catalyst fluidization.

CoO/MgO solid-solution catalysts exhibited similar catalytic performance to those of NiO/MgO [14,19]. For example, an effective 12 wt.% CoO/MgO solid-solution catalyst had a CO yield of 93% and a H_2 yield of 90% at the high space velocity of 60,000 ml (g of catalysts)$^{-1}$ h^{-1} and 1163 K, which remained unchanged during 50 h [14].

3. Inhibiting carbon deposition via formation of solid solution

Carbon formation can occur via two possible pathways in the CO_2 reforming of methane: CH_4 decomposition and CO disproportionation. The form of carbon on Ni or other metal surfaces generated during this reaction depends on the reaction conditions, namely, amorphous and filamentous carbons predominate in the lower temperature range of 623–873 K [21] and a graphitic structure at 973 K or higher temperatures [21,22].

Carbon deposition is dependent on both its thermodynamics and kinetics. Thermodynamic considerations suggest operation at high CO_2/CH_4 ratios (>1) and high temperatures to minimize carbon formation in the CO_2 reforming of methane [10,23]. However, a lower temperature and a CO_2/CH_4 ratio near unity are desirable for an industrial operation. Such an operation, which is thermodynamically favorable for carbon deposition, requires an effective catalyst that can kinetically inhibit the carbon formation. Two main properties of a catalyst affect the carbon deposition: surface structure and surface acidity [12]. Carbon deposition occurs more easily on larger nickel particles than smaller ones [24,25]. In other words, carbon deposition can be reduced or inhibited by decreasing metal particle sizes of catalysts. Furthermore, carbon deposition is favored by acidic supports. It has been suggested that carbon deposition can be attenuated or even suppressed when the metal is supported on a metal oxide with a strong Lewis basicity [13,26–28]. This occurs because the increase of the Lewis basicity of the support enhances the ability of the catalyst to chemisorb CO_2 in the CO_2 reforming of methane, and the adsorbed CO_2 reacts with C to form CO, resulting in the reduction of coke formation.

The formation of NiO–MgO (or CoO–MgO) solid solution provides an unique approach to inhibit carbon deposition. MgO is a strong Lewis base, which has a strong adsorption for CO_2 to reduce or inhibit carbon deposition. Furthermore, it was observed that the reduction of NiO or (CoO) in NiO–MgO (or CoO–MgO) solid solution was much more difficult than that of pure NiO (or pure CoO), leading to small nickel particles formed on the surface [12,13]. The combination of the surface basicity and the small metal particle size constitutes the ability of MgO-based solid-solution catalysts to inhibit carbon inhibition. Indeed, experimental results showed that both NiO/MgO and CoO/MgO solid-solution catalysts inhibited carbon deposition during CO_2 reforming of methane at atmospheric pressure [11–19].

It is worth noting that the high stability of NiO/MgO solid-solution catalyst for CO_2 reforming of methane at the atmospheric pressure was not maintained in the initial period of the reaction at a high pressure of 1.5 MPa (Fig. 2) [15a]. However, after the initial period, the catalyst got stabilized again at the high pressure (Fig. 2b). It was found that the amount of carbon deposits first increased with the reaction time at the high-pressure reaction and then remained unchanged. This indicates that the decrease in stability of the catalyst in the initial period is due to the carbon deposition. The carbon deposition did not continue after 12 h, leading to the re-stabilization of the catalyst. The re-stabilization was explained as the presence of two types of active sites for the reaction at the high pressure, namely, when the sites responsible for the carbon deposition become blocked, the formation of carbon deposits would stop increasing with the reaction time. Then, the other type of the metallic sites would function to give a stable activity for the reaction. The carbon deposition on NiO/MgO catalysts at high pressures can also be inhibited by fluidizing catalysts in the presence of O_2 [25b]. This happened because the deposited carbon was formed on the catalyst in oxygen-free reforming zone, and it was gasified in oxygen-rich zone by catalyst fluidization.

4. Isolation effect of solid-solution catalysts

From the above discussion, one can see that the formation of NiO–MgO (or CoO–MgO) solid solution makes NiO (or CoO) difficult to be reduced. In other words, only small amount of NiO (or CoO) in the solid solution can be reduced, leading to very small Ni (or Co) particles. The very small sizes of Ni (or Co) particles play an important role in inhibiting carbon deposition. However, so far, the reason why the formation of the solid solution makes the reduction of NiO (or CoO) so difficult is still unknown.

The reduction process of metal oxide (MO) can be expressed as

$$MO + H_2 = M + H_2O \quad (4)$$

It is generally accepted that the reduction of a metal oxide was controlled by the strength of M–O bond: the stronger the M–O

Table 1
Reduction temperatures of metal oxides and bond energies of metal oxides and metals.

Reduction	T (°C)[a]	E_{M-O} (kJ/mol)[b]	E_{M-M} (kJ/mol)[c]	ΔE (kJ/mol)[d]
PtO → Pt	−23	395	307	88
CuO → Cu	227	269	176	93
NiO → Ni	327	382	200	182
CoO → Co	377	384	167	217
MgO → Mg	No reduction	363	9	354

[a] Reduction temperatures of metal oxides by H_2 from Ref. [29].
[b] Bond strength of M–O from Ref. [30].
[c] Bond strength of M–M from Ref. [30].
[d] Strength difference between M–O and M–M bonds, i.e., $\Delta E = E_{M-O} - E_{M-M}$.

bond, the more difficult the reduction is. However, as shown in Table 1, one can see that the M–O bond strength of PtO is the largest among five metal oxides, but its reduction takes place at the lowest temperature. Although MgO occupies the second lowest M–O bond strength, it cannot be reduced even at a very high temperature. This indicates that the reduction of a metal oxide is not simply controlled by the strength of M–O bond. Actually, the energy change in the reduction of a metal oxide includes the break of the M–O bond (of metal oxide) and the H–H bond (of H_2) and the formation of the M–M (of solid metal) and the H–O bond (of H_2O). Because the break of the H–H bond and the formation of the H–O bond are the same for the reduction of all metal oxides, the difference in the reduction of various metal oxides is essentially dependent on the strengths of M–M and M–O bonds. The energy is required to break M–O bond of metal oxide, and the formation of the M–M bond of solid-metal product releases energy. It is reasonable to expect that the reduction should be proportional to the energy difference between M–O and M–M bonds instead of only the strength of M–O bond. Indeed, as shown in Table 1, the reduction temperature of metal oxides increases with the strength difference between M–O and M–M bonds. The bond strength of Mg–O (363 kJ/mol) is slightly lower than those of Ni–O (382 kJ/mol) and Co–O (384 kJ/mol), but the strength of Mg–Mg bond is only 9 kJ/mol, which is much lower than those of Ni–Ni (200 kJ/mol) and Co–Co (167 kJ/mol). This indicates that no reduction of MgO is mainly due to its too-low Mg–Mg bond strength. In other words, Ni–Ni (or Co–Co) bond formation plays a critical role in the reduction of NiO (or CoO). This can be further supported by the following Gibbs free energy changes. The Gibbs free energy change in the reduction of solid MgO to solid Mg is much larger than zero, whereas those of the reduction of solid NiO to solid Ni and the reduction of solid CoO to solid Co are negative (see Fig. 3). Those are consistent with the experimental results of TPR (temperature-programmed reduction) that the NiO and CoO can be reduced at 327 and 377 °C, respectively [12–14,29], but MgO cannot be reduced even at 1000 °C. In contrast, for the reduction of a metal oxide into its independent metal atom without M–M bonds, the Gibbs free energy change is much larger than zero for all three metal oxides (NiO, CoO, and MgO) (see Fig. 4). This obviously indicates that the reduction of NiO (or CoO) cannot take place without the formation of Ni–Ni (or Co–Co) bonds. In other words, the formation of Ni–Ni bonds is necessary during the reduction of NiO (see Fig. 5). This can allow us to answer the question "why does the formation of NiO–MgO solid solution create a difficulty for the reduction of NiO?". As shown in Fig. 6, there are two possible types of NiO species in the NiO–MgO solid solution: (1) NiO surrounded by MgO and (2) NiO surrounded by NiO. The first type of NiO cannot be reduced, because NiO is isolated by MgO, leading to impossibility to form Ni–Ni bond during removing O atom by hydrogen. In contrast, the reduction of the second type of NiO can take place (Fig. 6). This happens because the NiO is not isolated by

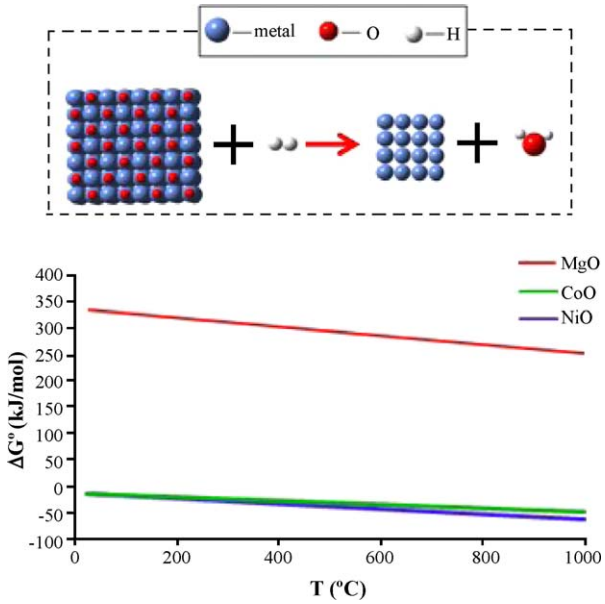

Fig. 3. The relationship between Gibbs free energy change (ΔG) and temperature (T) of solid metal oxide reduction with H_2 into H_2O and solid metal.

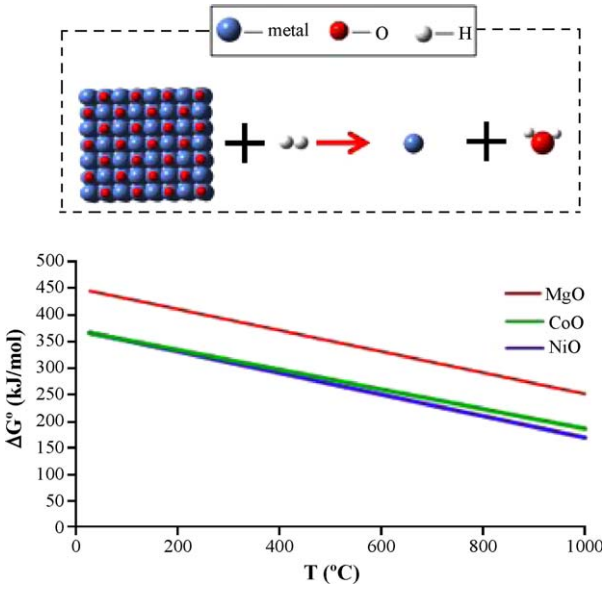

Fig. 4. The relationship between Gibbs free energy change (ΔG) and temperature (T) of solid metal oxide reduction with H_2 into H_2O and independent metal atom.

MgO and therefore Ni–Ni bond can be formed during removing O by hydrogen (Fig. 6). When NiO content is too low in NiO–MgO solid solution, NiO is mainly the first type that the NiO is surrounded by MgO. As a result, the NiO cannot be reduced. This is consistent with the experimental result that the 4.8 wt.% NiO/MgO solid-solution catalyst had a negligible activity for CO_2 reforming of methane, even after it was reduced by H_2 at a high temperature [12g]. In contrast, if NiO content is high, it has a high chance to form the second type that NiO is surrounded by NiO. Therefore, a large amount of NiO can be reduced to generate large Ni particles, which can cause carbon deposition. This would be the reason why the NiO/MgO solid-solution catalyst with a high content of NiO had a low stability [12g]. If the NiO content is neither too low nor too high in the solid solution, most of NiO should be the first type (NiO isolated by MgO) and the small part of NiO constitutes the second type (NiO surrounded by NiO), leading to the reduction of small

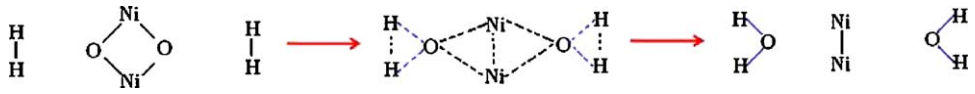

Fig. 5. Mechanism of NiO reduction by H_2.

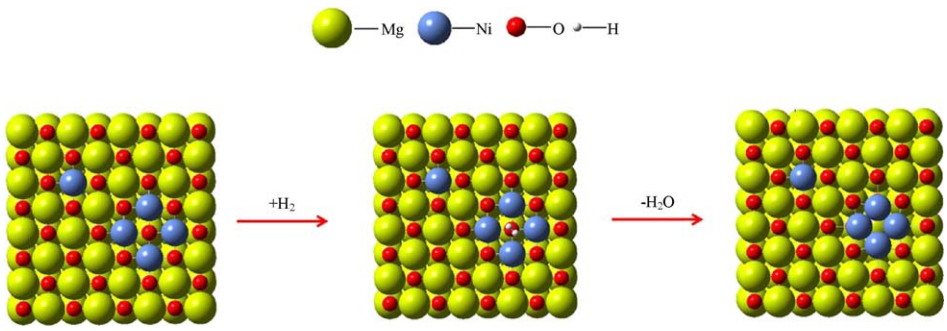

Fig. 6. The reduction of the NiO in a NiO–MgO solid solution (the first type of NiO species, which are surrounded by MgO, cannot be reduced, whereas the second type of NiO species, which are surrounded by NiO, can be reduced by H_2).

amount of NiO to generate very small particles, which contribute to the inhibition of carbon deposition. As a result, such a NiO–MgO solid solution with a suitable NiO content had an excellent stability with a high activity [12g]. Similarly, the isolation effect of solid solution can also be employed to explain the excellent catalytic performance of CoO/MgO solid-solution catalysts for CO_2 reforming of methane.

5. Summary

NiO–MgO (or CoO–MgO) solid solutions exhibited excellent activity and selectivity for CO_2 reforming of methane. Furthermore, the two properties of the solid-solution catalysts, the surface basicity and the small Ni (or Co) particles on the surface, constitute an unique resistance to carbon deposition, leading to a high stability for the reaction. The formation of small Ni (or Co) particles on the surface of the solid solution was attributed to the difficult reduction of NiO (or CoO) in the NiO–MgO (or CoO–MgO) solid-solution catalysts. Different from the general recognition that the reduction of a metal oxide is determined by its metal–oxygen bond strength, the reduction is strongly dependent on both metal–oxygen bond strength of metal oxide and the metal-metal bond strength of produced solid metal. Furthermore, the difficult reduction of NiO (or CoO) in the NiO–MgO (or CoO–MgO) solid-solution catalysts is due to the isolation effect that NiO (or CoO) is isolated by MgO, which inhibits the formation of the Ni–Ni (or Co–Co) bond during the reduction.

Appendix A. Calculation of Gibbs free energy change for metal oxide reduction

For the reduction of a metal oxide (Eq. (4)), the standard enthalpy and entropy changes at 298 K can be expressed as

$$\Delta H^0_{298} = \Delta H^0_{298,H_2O} + \Delta H^0_{298,M} - \Delta H^0_{298,MO} - \Delta H^0_{298,H_2} \quad \text{(A-1)}$$

$$\Delta S^0_{298} = S^0_{298,H_2O} + S^0_{298,M} - S^0_{298,MO} - S^0_{298,H_2} \quad \text{(A-2)}$$

According to the Neumann–Kopp Rule, Gibbs free energy change of metal oxide reduction can be expressed as

$$\Delta G^0_T = \Delta H^0_{298} - T\Delta S^0_{298} \quad \text{(A-3)}$$

where: T, reduction temperature; $\Delta H^0_{298,H_2O}$, standard molar enthalpy of H_2O formation at 298 K; $\Delta H^0_{298,H_2}$, standard molar enthalpy of H_2 formation at 298 K; $\Delta H^0_{298,MO}$, standard molar enthalpy of metal oxide formation at 298 K; $\Delta H^0_{298,M}$, standard molar enthalpy of metal formation at 298 K; S^0_{298,H_2O}, standard molar entropy of H_2O at 298 K; S^0_{298,H_2}, standard molar entropy of H_2 at 298 K; $S^0_{298,MO}$, standard molar entropy of metal oxide at 298 K; $S^0_{298,M}$, standard molar entropy of metal at 298 K; ΔH^0_{298}, standard molar enthalpy change of metal oxide reduction at 298 K; ΔS^0_{298}, standard molar entropy change of metal oxide reduction at 298 K; ΔG^0_T, standard molar Gibbs free energy change of metal oxide reduction at T.

Eq. (A-3) was used to plot Figs. 3 and 4. All standard molar enthalpies of compound formations and their standard molar entropies at 298 K were obtained from Ref. [30]. For the reduction of a metal oxide into solid metal, the standard enthalpy of solid-metal formation and its standard entropy were utilized. For the reduction of a metal oxide into an independent metal atom, the standard enthalpy of gaseous-metal formation and its standard entropy were employed.

References

[1] G.E. Keller, M.M. Bhasin, J. Catal. 73 (1982) 9.
[2] (a) R. Pitchai, K. Klier, Catal. Rev. Sci. Eng. 28 (1986) 13;
(b) N.R. Foster, Appl. Catal. A 19 (1985) 1;
(c) T.J. Hall, J.S.J. Hargreaves, G.J. Hutchings, R.W. Joyner, S.H. Taylor, Fuel Process. Technol. 42 (1995) 151.
[3] I. Pasquon, Plenary Lecture at EUOPACAT-1, Montpellier, France, 1–4 September, 1993.
[4] A.T. Ashcroft, A.K. Cheetham, J.S. Foord, M.L.H. Green, C.P. Grey, A.J. Murrell, P.D.F. Vernon, Nature 344 (1990) 319.
[5] (a) D.A. Hickman, L.D. Schmidt, J. Catal. 138 (1992) 267;
(b) D.A. Hickman, L.D. Schmidt, Science 259 (1993) 343;
(c) P. Torniainen, X. Chu, L.D. Schmidt, J. Catal. 146 (1994) 1.
[6] (a) V.R. Choudhary, A.M. Rajput, B. Prabhakar, Catal. Lett. 15 (1992) 363;
(b) V.R. Choudhary, A.M. Rajput, B. Prabhakar, J. Catal. 139 (1993) 326.
[7] Y.H.H.E. Ruckenstein, Adv. Catal. 48 (2004) 298.
[8] (a) X. Zhu, P.P. Huo, Y.P. Zhang, D.G. Cheng, C.J. Liu, Appl. Catal. B 81 (2008) 132;
(b) Y.X. Pan, C.J. Liu, L. Cui, Catal. Lett. 123 (2008) 96.
[9] J.P.J. Byrne, R.J. Gohr, R.T. Haslam, Ind. Eng. Chem. 24 (1932) 1129.
[10] A.M. Gadalla, B. Bower, Chem. Eng. Sci. 43 (1988) 3049.
[11] E. Ruckenstein, Y.H. Hu, Appl. Catal. A 133 (1995) 149.
[12] (a) Y.H. Hu, E. Ruckenstein, Catal. Rev. 44 (2002) 423;
(b) Y.H. Hu, E. Ruckenstein, J. Phys. Chem. B 101 (1999) 7563;
(c) E. Ruckenstein, Y.H. Hu, Catal. Lett. 51 (1998) 183;
(d) Y.H. Hu, E. Ruckenstein, Catal. Lett. 43 (1997) 71;
(e) E. Ruckenstein, Y.H. Hu, Appl. Catal. A 154 (1997) 185;
(f) E. Ruckenstein, Y.H. Hu, J. Catal. 162 (1996) 230;

(g) Y.H. Hu, E. Ruckenstein, Catal. Lett. 36 (1996) 145;
(h) Y.H. Hu, E. Ruckenstein, J. Catal. 184 (1999) 298;
(i) Y.H. Hu, E. Ruckenstein, J. Catal. 163 (1996) 306;
(j) Y.H. Hu, E. Ruckenstein, Langmuir 13 (1997) 2055.
[13] (a) K. Tomishige, Y. Himeno, Y. Matsuo, Y. Yoshinaga, K. Fujimoto, Ind. Eng. Chem. Res. 39 (2000) 1891;
(b) Y.G. Chen, K. Tomishige, K. Yokoyama, K. Fujimoto, J. Catal. 184 (1999) 479;
(c) K. Tomishige, O. Yamazaki, Y. Chen, K. Yokoyama, X. Li, K. Fujimoto, Catal. Today 45 (1998) 35;
(d) Y. Chen, K. Tomishige, K. Fujimoto, Chem. Lett. (1997) 999;
(e) Y. Chen, K. Tomishige, K. Yokoyama, K. Fujimoto, Appl. Catal. A 165 (1997) 335;
(f) Y.G. Chen, K. Tomishige, K. Fujimoto, Appl. Catal. A 161 (1997) L11;
(g) O. Yamazaki, T. Nozaki, K. Omata, K. Fujimoto, Chem. Lett. (1992) 1953.
[14] (a) E. Ruckenstein, H.Y. Wang, J. Catal. 205 (2002) 289;
(b) E. Ruckenstein, H.Y. Wang, Catal. Lett. 73 (2001) 99;
(c) E. Ruckenstein, H.Y. Wang, Appl. Catal. A 204 (2000) 257.
[15] (a) Y.H. Wang, B.Q. Xu, Catal. Lett. 99 (2005) 89;
(b) Y.H. Wang, H.M. Liu, B.Q. Xu, J. Mol. Catal. A 299 (2009) 44.
[16] A. Djaidja, S. Libs, A. Kiennemann, A. Barama, Catal. Today 113 (2006) 194.
[17] C.S. Song, P. Wei, Catal. Today 98 (2004) 463.
[18] K. Tomishige, Catal. Today 89 (2004) 405.
[19] (a) V.R. Choudhary, A.S. Mamman, Appl. Energy 66 (2000) 161;
(b) V.R. Choudhary, A.S. Mamman, J. Chem. Technol. Biotechnol. 73 (1998) 345;
(c) K.C. Mondal, V.R. Choudhary, U.A. Joshi, Appl. Catal. A 316 (2007) 47.
[20] Y. Pan, C.J. Liu, Q. Ge, Langmuir 24 (2008) 12410.
[21] (a) R.T.K. Baker, P.S. Harris, Chemistry and Physics of Carbon, vol. 14, Dekker, New York, 1979, p. 83;
(b) W. Baukloh, B. Chatterjee, P.P. Das, Trans. Indian Inst. Metals 4 (1950) 271;
(c) V.J. Kehrer, H. Leidheiser Jr., J. Phys. Chem. 58 (1954) 550;
(d) J.R. Rostrup-Nielsen, J. Catal. 27 (1972) 343.
[22] (a) G.D. Renshaw, C. Roscoe, P.L. Walker, J. Catal. 22 (1971) 394;
(b) H.E. Grenga, K.R. Lawless, J. Appl. Phys. 43 (1972) 1508;
(c) G.D. Renshaw, C. Roscoe, P.L. Walker, J. Catal. 18 (1970) 164.
[23] (a) R.E. Reitmeier, K. Atwood, H.A. Bennet Jr., H.M. Baugh, Ind. Eng. Chem. 40 (1948) 620;
(b) G.A. White, T.R. Roszkowski, D.W. Stanbridge, Hydrocarbon Process. 54 (1975) 130.
[24] J.R. Rostrup-Nielsen, J. Sehested, J.K. Norskov, Adv. Catal. 47 (2002) 65.
[25] (a) K. Tomishige, Y.G. Chen, K. Fujimoto, J. Catal. 181 (1999) 91;
(b) K. Tomishige, Y. Matsuo, Y. Yoshinaga, Y. Sekine, M. Asadullah, K. Fujimoto, Appl. Catal. A 223 (2002) 225.
[26] Z.L. Zhang, X.E. Verykios, Catal. Today 21 (1994) 589.
[27] T. Horiuchi, K. Sakuma, T. Fukui, Y. Kubo, T. Osaki, T. Mori, Appl. Catal. A 144 (1996) 111.
[28] G.J. Kim, D.S. Cho, K.-H. Kim, J.H. Kim, Catal. Lett. 28 (1994) 41.
[29] C.W. Chou, S.J. Chu, H.J. Chiang, C.Y. Huang, C.J. Lee, S.R. Sheen, T.P. Perng, C.T. Yeh, J. Phys. Chem. B 105 (2001) 9113.
[30] D.R. Lide (Ed.), CRC Handbook of Chemistry and Physics, 81th edition, CRC Press, 2001.